Materials Advances

ROYAL SOCIETY OF CHEMISTRY

PAPER

View Article Online
View Journal | View Issue

Cite this: *Mater. Adv.*, 2023, 4, 1515

Discrimination and detection of NO_2, NH_3 and H_2S using sensor array based on three ambipolar sandwich tetradiazepinoporphyrazinato/phthalocyaninato europium double-decker complexes†‡

Xia Kong, §[ab] Ekaterina N. Tarakanova, §[cd] Xiaoli Du,§[be] Larisa G. Tomilova[d] and Yanli Chen *[b]

Developing a room-temperature operated gas sensor for highly efficient discrimination of various toxic gases, is highly desirable but remains challenging to date. Herein, the successful development of a novel sensor array is reported, which discriminates between three gases using solution-based quasi-Langmuir–Shäfer (QLS) films from three ambipolar sandwich tetradiazepinoporphyrazinato/phthalocyaninato europium double-decker complexes [^{nBu}Pc]$_2$Eu (**1**), [^{tBuPh}DzPz][^{nBu}Pc]Eu (**2**) and [^{tBuPh}DzPz]$_2$Eu (**3**). For the three oxidizing and reducing gases: NO_2, NH_3, H_2S at the sub-ppm level, **1** showed a response to NO_2 and NH_3, **2** responded to the three gases, and **3** responded to NO_2 and H_2S. Because of the synergistic effect between film-conductivity from the highly conjugated phthalocyanine ligands and the effective binding sites from the diazepine moieties, the QLS film **2** showed the best gas-sensing performance of all the sensors in terms of both sensing response to the three toxic gases, and the highest sensitivities (% ppm^{-1}) of 46.84, 0.39 and 2.34 for NO_2, NH_3 and H_2S, respectively. Furthermore, by combining the distinct response patterns of the devices, a sensor array was established to qualitatively and quantitatively distinguish NO_2, NH_3 and H_2S gases with ultralow detection concentrations (20 ppb of NO_2, 1 ppm of NH_3 and 100 ppb of H_2S), with a fast response time (1 min) and good stability at room temperature.

Received 29th November 2022,
Accepted 4th February 2023

DOI: 10.1039/d2ma01058e

rsc.li/materials-advances

Introduction

High-precision gas sensors are essential in modern society for detecting various hazardous gases, such as H_2S, NO_2, NH_3, toluene, benzene, and so on.[1] Researchers are at the early stages of developing various gas sensing devices based on inorganic semiconducting materials, which are generally operated at higher working temperatures.[2] Higher working temperatures will not only lead to a significant increase in energy consumption, as well as destruction of the microstructure of the sensing nanomaterial, but are also dangerous for detecting flammable and explosive gases. As a result, while developing a room-temperature operated gas sensor for highly efficient discrimination of various toxic gases is highly desirable, it remains a challenge.

As is already known, active sensing semiconductor materials,[3] the optimized microstructure of the active layers[4,5] and advanced device preparation[6,7] usually achieve a good sensing performance with a high sensitivity and selectivity. Among the sensing semiconductor materials, the sandwich-type phthalocyanine family has attracted extensively research interest because of the excellent charge transport properties, easy modulation of the frontier molecular orbital energy levels, and quite good solubility in common organic solvents[8–11] which allow low-cost and large-area devices to be fabricated by solution-based methods such as spin coating,[12] molecular

[a] *College of Chemical and Biological Engineering, Shandong University of Science and Technology, Qingdao 266590, P. R. China. E-mail: kongxia_chem@sdust.edu.cn*
[b] *School of Materials Science and Engineering, Institute of Advanced Materials, China University of Petroleum (East China), Qingdao 266580, P. R. China. E-mail: yanlichen@upc.edu.cn*
[c] *Ivanovo State University of Chemistry and Technology, RF-153000 Ivanovo, Russian Federation*
[d] *Institute of Physiologically Active Compounds at Federal Research Center of Problems of Chemical Physics and Medicinal Chemistry, Russian Academy of Sciences, 1 Severny Proezd, 142432 Chernogolovka, Russian Federation*
[e] *Key Laboratory for Organic Electronics and Information Displays (KLOEID), Institute of Advanced Materials (IAM), Nanjing University of Posts & Telecommunications, 9 Wenyuan Road, Nanjing 210023, P. R. China*

† This manuscript is dedicated to the memory of our friend Professor Larisa G. Tomilova.

‡ Electronic supplementary information (ESI) available. See DOI: https://doi.org/10.1039/d2ma01058e

§ These authors contributed equally to this work.

assemblies,[13] Langmuir,[14,15] and quasi-Langmuir–Shäfer (QLS) techniques,[16] and so on. Moreover, it is well-known that sandwich phthalocyaninato rare earth double-decker complexes with a radical nature, and extended π networks along the axis perpendicular to the macrocycle plane,[17] are expected to play a more important part in chemical sensing applications,[18,19] data storage[20] and field-effect transistors[21,22] than their monomeric counterparts. For example, the solution-processed thin solid films of amphiphilic bis(phthalocyaninato) rare earth double-deckers, HoPc[Pc(OPh)$_8$] and Ho[Pc(OPh)$_8$]$_2$, have been revealed to display sensitive responses to reducing NH_3 gas, and found that the introduction of electron-withdrawing substituents on the periphery of the phthalocyanine rings can improve the response of the organic materials.[23]

Diazepine heterocycles with promising biological activities, are present in a wide range of numerous bioactive molecules, pharmaceuticals, and natural products. Recently, it was found that the presence of the substituents for diazepine heterocycles can increase effective active sites used in the heterogeneous catalyst for C–C coupling reactions,[24,25] phosphorescent organic light-emitting diodes (OLEDs),[26] catalysis and bioorganometallic chemistry[27] and so on. Thus, in the present study, three heteroleptic and homoleptic sandwiched complexes: bis(phthalocyaninato)europium [$^{n\mathrm{Bu}}$Pc]$_2$Eu (**1**), the mixed (phthalocyaninato)(tetradiazepinoporphyrazinato)europium [$^{t\mathrm{BuPh}}$DzPz][$^{n\mathrm{Bu}}$Pc]Eu (**2**), and the bis(tetradiazepinoporphyrazinato)europium [$^{t\mathrm{BuPh}}$DzPz]$_2$Eu (**3**) [$^{n\mathrm{Bu}}$Pc = 2,3,9,10,16,17,23,24-octabutylphthalocyaninate, $^{t\mathrm{BuPh}}$DzPz = tetrakis(5,7-bis(4-*tert*-butylphenyl)-6*H*-1,4-diazepino)[2,3-*b*,*g*,*l*,*q*]porphyrazinate] (Fig. 1), were synthesized according to previously described procedures,[28–30] and fabricated into well-organized films by QLS method. Exposing the active layers of films **1–3** to the three sub-ppm level gases (NO_2, NH_3, H_2S) at room temperature, various responses of the active layers to the three gases were obtained. By combining the distinct response patterns of **1–3**, a sensor array was constructed to distinguish between these three toxic gases. The present work, represents continuous efforts to understand the relationship between the film structure, morphology and gas sensor performance of the tetrapyrrole organic semiconductors,[18,19,23,31] and will be useful for attracting further research interest in the field of chemical sensors, especially gas sensor applications based on double-decker phthalocyaninato rare earth complexes.

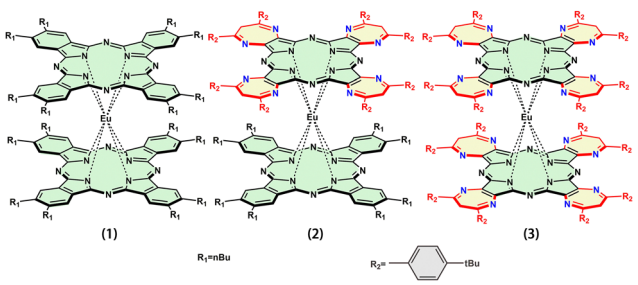

Fig. 1 Schematic molecular structures of [$^{n\mathrm{Bu}}$Pc]$_2$Eu (**1**), [$^{t\mathrm{BuPh}}$DzPz][$^{n\mathrm{Bu}}$Pc]Eu (**2**) and [$^{t\mathrm{BuPh}}$DzPz]$_2$Eu (**3**).

Results and discussion

Electronic absorption spectra

The electronic absorption spectra of the double-decker compounds **1–3** were recorded in dichloromethane (DCM) solution (Fig. 2), and the corresponding data are compiled in Table S1 (ESI‡). The spectra show intense Soret bands in the range of 320–360 nm, and an intense Q-band, at 685 nm for **1**, two broadened Q-bands at 640 and 698 nm for **2**, and at 631 and 696 nm for **3**, which were attributed to the π–π* transitions.[23,29,30] Unlike [$^{n\mathrm{Bu}}$Pc]$_2$Eu (**1**) with a free radical peak at 492 nm, confirming its π-radical nature, the isolated double-deckers **2** and **3** existed

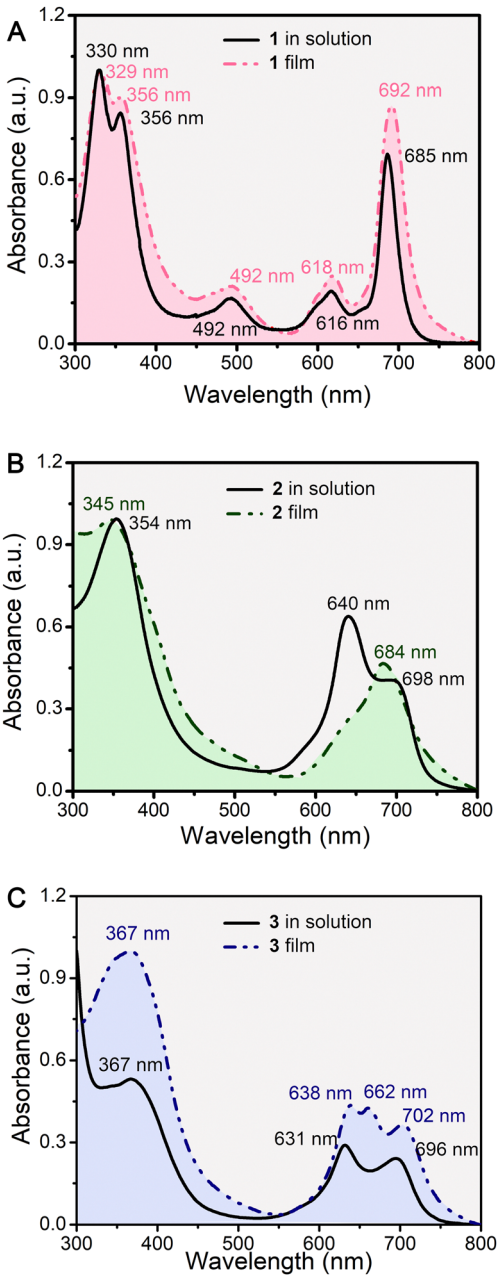

Fig. 2 Electronic absorption spectra of **1–3** (A–C) in DCM solution (solid line) and the QLS films (dashed line).

in the DCM solution in their anionic forms as reported previously.[28–30] Gradually replacing the [$^{n\mathrm{Bu}}$Pc] ligand by [$^{t\mathrm{BuPh}}$DzPz] from [$^{n\mathrm{Bu}}$Pc]$_2$Eu (**1**) to [$^{t\mathrm{BuPh}}$DzPz][$^{n\mathrm{Bu}}$Pc]Eu (**2**) and [$^{t\mathrm{BuPh}}$DzPz]$_2$Eu (**3**), the splitting of the Q-band in the spectrum of the anionic form increased from 0 nm for **1**, 58 nm for **2** to 65 nm for **3**, reflecting the enhanced intramolecular π–π interactions between the macrocycles provided by the diazepine moieties.[29] After fabrication into the QLS films, the electronic absorption spectra at 450–500 nm of **1–3** were essentially unchanged, which inferred that the [$^{n\mathrm{Bu}}$Pc]$_2$Eu (**1**) still had a π-radical nature, and [$^{t\mathrm{BuPh}}$DzPz][$^{n\mathrm{Bu}}$Pc]Eu (**2**) and [$^{t\mathrm{BuPh}}$DzPz]$_2$Eu (**3**) were still anionic in nature.[30] However, it is worth noting that the main Q band, the most intense, was red-shifted from 685 to 692 nm (7 nm) for **1**, from 640 to 684 nm (44 nm) for **2**, and from 631 to 638 nm (7 nm) for **3**, indicating the formation of *J* aggregates in the multilayers due to the strong exciton coupling and a very strong interaction between the neighboring molecules in one layer.[32] In addition, a remarkable red-shift of the Q band in the QLS films of the heteroleptic **2** compared to homoleptic **1** and **3** was observed, indicating that stronger intermolecular interactions between the neighboring double-decker molecules existed in film **2** than those of both **1** and **3**. These results revealed that the degree of symmetry in molecule structure had a great influence on the intermolecular interaction in solid films.

X-ray diffraction

To obtain information about the microstructure, X-ray diffraction (XRD) patterns of the QLS films **1–3** were recorded. As shown in Fig. 3, the QLS film **1** shows three well-defined diffraction peaks at 2θ = 4.86° (1.82 nm), 9.48° (0.93 nm) and 14.0° (0.63 nm), which were ascribed to the diffractions from the (001), (002) and (003) planes, respectively. This indicated that the QLS film **1** consisted of the regular repeating unit (actually a long-range molecular order) across the *c*-axis of the unit cell (*i.e.*, the direction perpendicular to the tetrapyrrole rings).[33,34] The average *d* space calculated according to the Bragg equation was about 1.86 nm and corresponded to the distance between two adjacent molecules of [$^{n\mathrm{Bu}}$Pc]$_2$Eu (**1**) in the direction perpendicular to the tetrapyrrole rings. In the wide-angle region, an additional diffraction at 0.31 nm was present, which was attributed to the π–π stacking distance between the tetrapyrrole cores of neighboring double-decker molecules. As is already known, the good molecular ordering with intensive intra/intermolecular π–π interactions is certainly expected to enhance the capacity of charge transfer for the semiconducting layers, which was verified again in a current–voltage test (*vide infra*).[23] For films **2** and **3**, the (001) Bragg peak of the films occurred at *ca.* 4.37° and 5.53°, respectively, resulting in layer spaces of 2.02 nm for **2** and 1.94 nm for **3**. The QLS films of both **2** and **3** also exhibited diffraction at 0.31 nm from the π–π stacking between the tetrapyrrole cores of neighboring double-decker molecules. Judging by the diagonal dimensions of the **1–3** molecules, 2.51, 2.90 and 2.94 nm, respectively, the orientation angle between the phthalocyanine ring of the double-decker molecule and the substrate surface was calculated as *ca.* 47.8°, *ca.* 44.2°, *ca.* 41.3° for **1**, **2** and **3**, respectively. This was in agreement with the calculated results based on the polarized

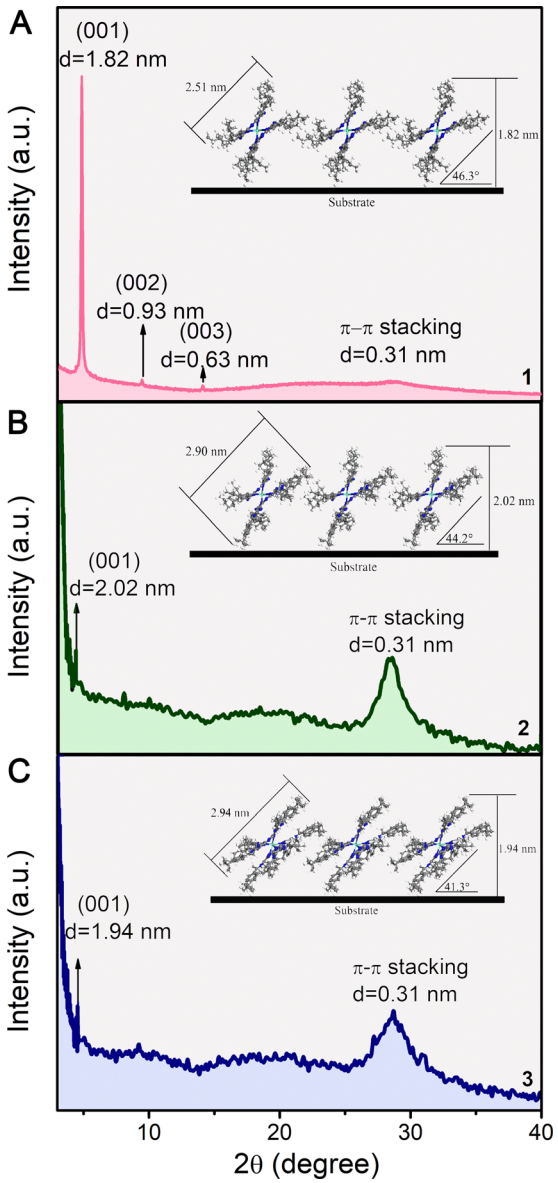

Fig. 3 The X-ray diffraction patterns of the QLS films of compounds **1–3** (A–C) and schematic representations of the QLS films of **1–3** (insets of A–C).

UV-vis spectroscopy, 48.4°, 44.3°, 38.4° for **1**, **2** and **3**, respectively,[35] (see Fig. S1 and Table S2, ESI‡). Consequently, the orientation of the double-decker molecules in films **1–3** were nearly parallel to the substrate surface in the *J*-aggregation mode with an "edge-on" conformation (see insets of Fig. 3). Moreover, a comparison of the (001) diffraction peaks for the QLS films **1–3** in the XRD patterns revealed that the lower film-crystallinity of **2** and **3**, was probably due to the substituents of diazepine heterocycles introduced into the periphery of the tetrapyrrole ring, and the lowest film crystallinity, would negatively impact on the charge transport.

SEM surface topography

In order to observe the surface morphology of the films **1–3**, the scanning electron microscopy (SEM) was used. As shown in

Fig. S2 (ESI‡), a well-defined membrane structure with a gradually reduced nanoparticle size from **1** to **2** and **3** was observed on the respective QLS films, with the smallest nanoparticles achieved for **3**. From the nanoparticles formed in the QLS films, the film crystallinity increased in the order of **1** > **2** > **3**, which was consistent with the results of the XRD patterns and a previous report,[24] further confirming the negative effect of diazepine heterocycles on the crystallinity of the molecular aggregates. It is worth noting that the smaller the particles, the larger the specific surface area, and the more binding sites, which is favorable for combining the gas molecules, and thus, facilitates the gas-sensing performance.

Ultraviolet photoelectron spectroscopy (UPS) analysis

To obtain the energy levels of the QLS films **1–3**, UPS analysis and vis-NIR absorption spectra were recorded (see Fig. S3, ESI‡). He I (21.22 eV) was used as the energy source in the UPS analysis. According to the method in the literature,[36] the HOMO and LUMO energy levels of the films **1–3** were estimated to be about −5.69 and −4.42 eV for **1**, −4.35 and −3.33 eV for **2**, and −4.36 and −3.23 eV for **3**, respectively, which simultaneously have the energy range required for p-type and n-type organic semiconductors,[37–39] indicating the ambipolar semiconducting nature of these three sandwich tetradiazepinoporphyrazinato/phthalocyaninato europium double-decker complexes. The potential gap was in good agreement with results from the literature, 1.27, 0.99, 1.12 eV for [$^{n\mathrm{Bu}}$Pc]$_2$Eu (**1**), [$^{t\mathrm{BuPh}}$DzPz][$^{n\mathrm{Bu}}$Pc]Eu (**2**) and [$^{t\mathrm{BuPh}}$DzPz]$_2$Eu (**3**), respectively.[29,30]

Current–voltage (*I–V*) characteristics

In order to determine the conductivity of materials, the current–voltage (*I–V*) curves were measured. As shown in Fig. 4, all the devices exhibited good Ohmic behavior at a low bias voltage, which confirmed the good electrical contact between the organic self-assemblies and electrodes. Furthermore, the current increased in the order of film **1** > film **2** > film **3**. The estimated electronic conductivity (σ) was about 6.84×10^{-5}, 3.90×10^{-5} and 8.63×10^{-6} S cm^{-1} for the QLS films **1**, **2** and **3**, respectively. The highest film conductivity was found for complex **1** and should be attributed to highest ordered molecular arrangement and immediate π-stacking with the adjacent [$^{n\mathrm{Bu}}$Ph]$_2$Eu molecules. Conversely, complex **3** having the largest number of diazepine heterocycles showed the lowest conductivity, which indicated that the number of diazepine heterocycles played a critical role in tuning the intermolecular stacking, which then impacted on the electrical conductivity of the materials.

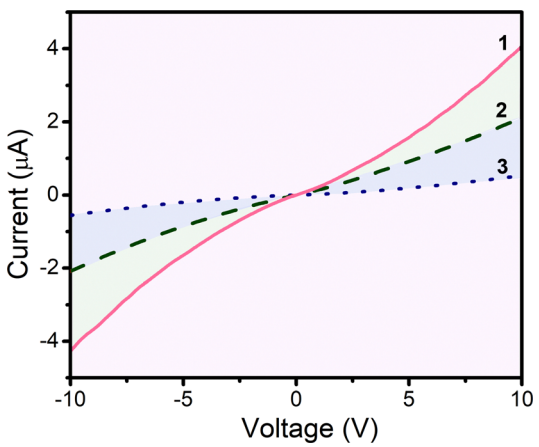

Fig. 4 Representative *I–V* curves of the QLS films of compounds **1–3**.

Sensor performance measurements

To assess the applicability of the gas sensing properties, the gas sensing response was determined from the change of current before and after gas injection. Fig. 5 shows the dynamic curves of the current change of the devices fabricated on QLS films **1–3** before and after injection of 20–900 ppb NO_2, 1–12.5 ppm NH_3, and 100–600 ppb H_2S in a N_2 atmosphere at room temperature. The original experimental curves are shown in Fig. S4 (ESI‡). The dynamic exposure period was fixed at 1 min (with a 1–2 min full recovery times) for all three gases. As shown in the Fig. 5A–C, the current of the QLS films **1–3** decreased when the NO_2 gases contacted with the sensor, and increased during recovery, which was consistent with the n-type sensing behavior previous reported in the literature.[40,41] Interestingly, when the electron-donating gas NH_3 (1–12.5 ppm), contacted with the sensors, the current of QLS films **1** and **2** still decreased, and in an H_2S (100–600 ppb) atmosphere, the current of QLS films **2** and **3** decreased. This can be explained by the fact that when the NO_2 molecules of the oxidizing gas were adsorbed on the surface of the semiconducting active layer as the electron acceptors, the density of the positive charge carriers increased, resulting in a current decrease for the n-type semiconductor. For the reducing gases, NH_3 and H_2S, the electrons will combine with the holes, resulting in a current decrease for the p-type semiconductor.[18,42,43] Therefore, the ambipolar (n- and p-type) response to the oxidizing NO_2 and the reducing NH_3 and H_2S was revealed for films **1–3**, which was consistent with the results of the UPS analysis.

The relative response was calculated for each concentration in order to quantitatively determine the sensor responses by using the following expression:

$$\mathrm{RR}(\%) = [(I_0 - I_f)/I_0] \times 100$$

where I_0 is the original current value before gas injection, and I_f is the current value at the end of the 1 min exposure period. As shown in Fig. 6, the sensor response of QLS films **1–3** were all linear with concentrations of NO_2, NH_3 and H_2S in the ranges of 20–900 ppb, 1–12.5 ppm and 100–600 ppb, respectively. The adjusted R^2 were all larger than 0.97. Thus, such films could be used to determine the concentration of the three gases quantitatively. The sensitivities of QLS films **1**, **2** and **3** were calculated using the slope of the curve (in % ppm^{-1}) of the linear fit, and were about 26.70, 46.84 and 18.31 for NO_2, 0.20, 0.39 and 0 for NH_3, and 0, 2.34, 1.62 for H_2S, respectively, which is summarized in Table S3 (ESI‡). As is already known, NO_2 is a strong oxidizing agent, which can directly neutralize the negative free charge carriers in the material. The response is very sensitive and the detection limit is relatively low. In contrast, the H_2S

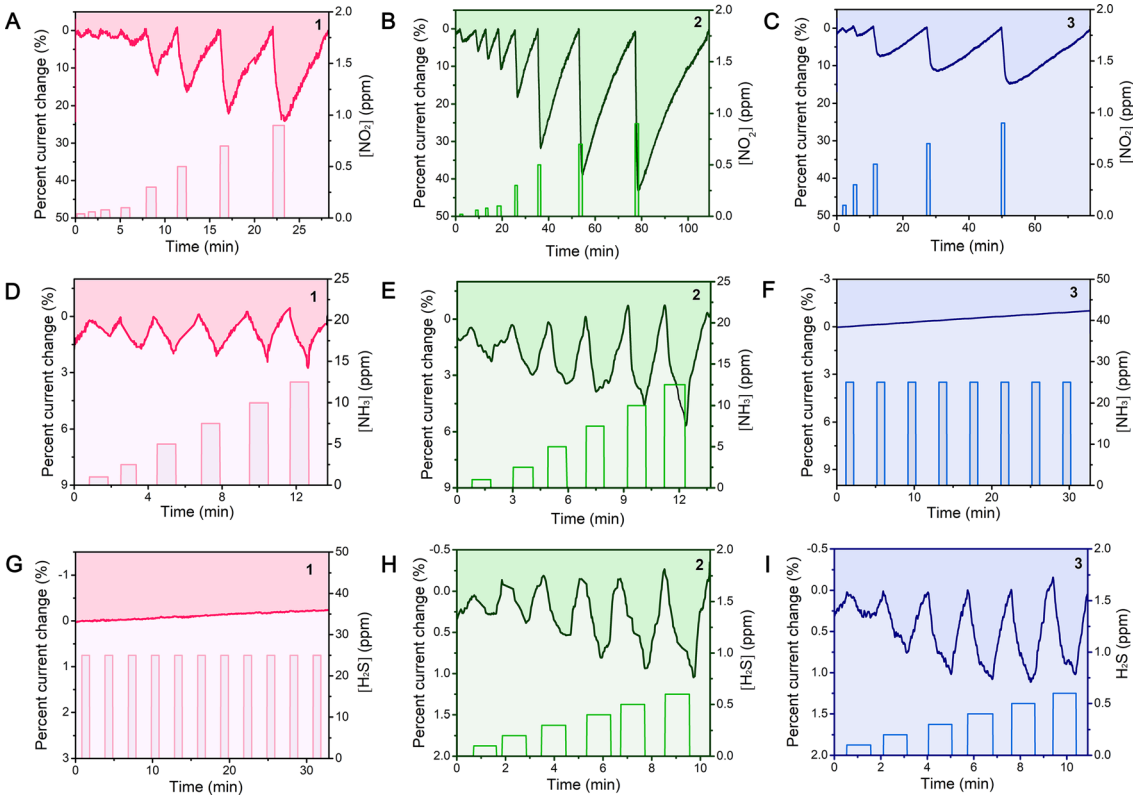

Fig. 5 The time-dependent current plots for the QLS films of compounds **1–3** (A–I) exposed to toxic gases at various concentrations (exposure: 1 min), while the bottom rectangular pulses for each current plot represent the gas concentration as a function of time. A, B and C is exposure to the oxidizing gas NO_2 in the range of 20–900 ppb, D, E and F is exposure to the reducing gas NH_3 in the range of 1–12.5 ppm, and G, H and I is exposure to the reducing gas H_2S in the range of 100–600 ppb.

and NH_3 interact with the nitrogen atoms of the diazo compounds by an acid–base interaction, and the different strengths of the interaction forces lead to different sensitivities and detection limits. Impressively, QLS film **2**, because of a moderate film-crystallinity, conductivity and binding sites, showed a more superior sensing response than those of **1** and **3** for the detection of both the oxidizing gas NO_2 and the reducing gases NH_3 and H_2S. Meanwhile the QLS film **1** with the highest film-crystallinity and conductivity exhibited a higher response towards NO_2 and NH_3, than those of **3**, but a negligible response to H_2S. Despite the poor film-crystallinity and conductivity, QLS film **3** with the larger number of diazepine heterocycles showed a response to both NO_2 and H_2S, but not to NH_3. This indicated that the diazepine rings from the double-decker possessed basic electron-rich nitrogen centers that bind more strongly to the partially acidic NO_2 and H_2S gases. It was apparent that the observed various responses to the three toxic gases indicated that the synergistic effect between film-crystallinity/conductivity and binding sites imparted the best gas-sensing performance of QLS film **2** in terms of both sensing response to the three gases and the highest sensitivity films of **1–3**.

Sensor array construction

As reported previously, the conductivity of films **1–3** were all decreased during exposure to both oxidizing and reducing gases, which was an obstacle to specifically discriminating these three gases (NO_2, NH_3 and H_2S). However, from the response selectivity of compounds **1–3**, a sensor array was constructed to distinguish between these three toxic gases. It was very easy to clearly distinguish three gases according to the qualitative current change map shown in Table S4 (ESI‡), where a green spot represents the current decrease, and a red spot represents a poor current change. It was easily inferred that much larger current decrease from sensors **1–3** with three green spots meant that the atmosphere was NO_2, and the poor current change with the red spot of **3** meant NH_3 gas, and of **1** meant H_2S gas. Meanwhile, according to the comparison of recently reported sensor arrays[44,45] listed in Table S5 (ESI‡), the sensing array fabricated in this research shows promise for use in room-temperature detection and discrimination of ultra-low concentrations of NO_2, NH_3 and H_2S gases.

The stability of the sensors to the three toxic gases should be concerned in order to improve the future practical applications. As shown in Fig. S5 (ESI‡), all three devices show excellent stable sensing behavior and the quite good reproducibility ($\sim$500 ppb NO_2, 12.5 ppm NH_3 and 300 ppb H_2S) after five cycling tests. Furthermore, the concentration detection range for the three toxic gases have also met the required standard for outdoor air quality control and public health (39–117 ppb NO_2, 1.3–6.6 ppm NH_3 and 20–395 ppb H_2S) in China and the USA,[46] which suggests the highly practical application potential of the present sensor array in quantitatively determining air pollutants.

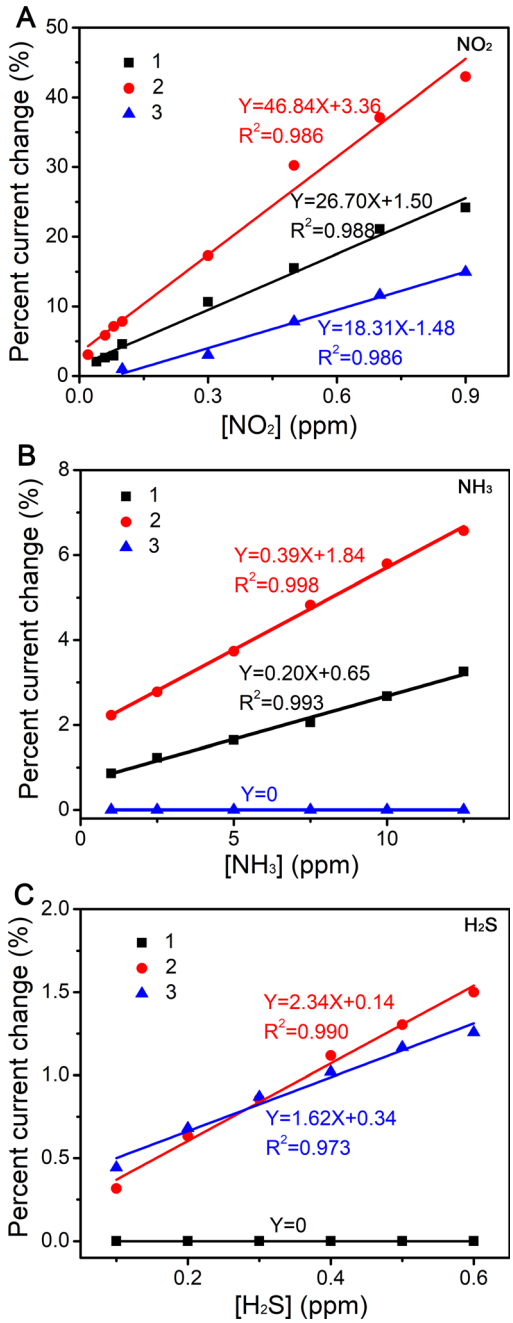

Fig. 6 Sensor response varies linearly with the NO_2, NH_3 and H_2S concentrations of the QLS films of compounds **1–3**. The slope (% ppm^{-1}, $R^2 \geq 0.97$) for each may be used as a measurement of the sensitivity of the sensor.

Conclusions

The QLS films **1–3** used as chemiresistive sensors, exhibited a sensitive response to NO_2, NH_3 and H_2S in the 20–900 ppb, 1–12.5 ppm, 100–600 ppb ranges, respectively, with the sensor responses obeying first-order analyte-film interaction kinetics. According to the different sensing behaviors of QLS films **1–3**, a sensor array was constructed to discriminate between the oxidizing gas (NO_2) and the reducing gases (NH_3 and H_2S) with high sensitivity, high selectivity and excellent reversibility and reproducibility even at room temperature, showing the promising practical application potential of the present sensor array in quantitatively determining air pollutants. It was found that an ingenious combination of the diazepine heterocycles possessing effective active sites to bind analytes, and the phthalocyaninato ligand having a large conjugated π-system to promote the charge transport, play a decisive role for the improvement of sensing performance of the organic semiconducting molecules. The present study not only presents a promising sensor array for the room-temperature detection and discrimination of ultra-low concentrations of NO_2, NH_3 and H_2S gases by using ambipolar organic semiconductors, but more importantly provides a new way for the preparation of high-performance sensor devices with a combination of a reasonable molecular design and a low-cost, self-assembly device fabrication technique.

Author contributions

Xia Kong: methodology, experiment, writing – original draft. Ekaterina N. Tarakanova: synthesis of compounds. Xiaoli Du: methodology, experiment, writing. Yanli Chen: writing – review and editing, funding acquisition, supervision.

Conflicts of interest

There are no conflicts to declare.

Acknowledgements

This work was financially supported by the National Natural Science Foundation of China (Grant No. 21771192, 22001150), the Natural Science Foundation of Shandong Province (Grant No. ZR2017ZB0315, ZR2020QB029), the Fundamental Research Funds for the Central Universities (Grant No. 18CX06001A, 18CX02053A, 19CX05001A), Postgraduate's Innovation Project (Grant No. YCX2019070), RFBR (Project number 19-33-60099, ENT) and the State Assignment of 2022 (Grant No. FFSN-2021-0003). We are especially grateful to Professor Larisa G. Tomilova, founder of the native Phthalocyanine School, who unexpectedly passed away on the 4th of January 2021 fighting the COVID-19 disease. Larisa Tomilova was a very intelligent and hardworking person. Her strong contribution to phthalocyanine research will be greatly missed. This paper is dedicated to her memory.

References

1 Z. Li, H. Li, Z. Wu, M. Wang, J. Luo, H. Torun, P. Hu, C. Yang, M. Grundmann, X. Liu and Y. Fu, Advances in designs and mechanisms of semiconducting metal oxide nanostructures for high-precision gas sensors operated at room temperature, *Mater. Horiz.*, 2019, **6**, 470–506.
2 A. Chidambaram and K. C. Stylianouk, Electronic metal–organic framework sensors, *Inorg. Chem. Front.*, 2018, **5**, 979–998.

3 W. Yang, L. Gan, H. Li and T. Zhai, Two-dimensional layered nanomaterials for gas-sensing applications, *Inorg. Chem. Front.*, 2016, **3**, 433–451.
4 A. Kumar, N. A. Mejjati, R. Meunier-Prest, A. Krystianiak, O. Heintz, E. Lesniewska, C. H. Devillers and M. Bouvet, Tuning of interfacial charge transport in polyporphine/phthalocyanine heterojunctions by molecular geometry control for an efficient gas sensor, *Chem. Eng. J.*, 2022, **429**, 132453.
5 Y. Chen, M. Bouvet, T. Sizun, G. Barochi, J. Rossignol and E. Lesniewska, Enhanced chemosensing of ammonia based on the novel molecular semiconductor-doped insulator (MSDI) heterojunctions, *Sens. Actuators, B*, 2011, **155**, 165–173.
6 N. S. Nikolaeva, D. D. Klyamer, S. M. Zharkov, A. R. Tsygankova, A. S. Sukhikh, N. B. Morozova and T. V. Basova, Heterostructures based on Pd–Au nanoparticles and cobalt phthalocyanine for hydrogen chemiresistive sensors, *Int. J. Hydrogen Energy*, 2021, **46**, 19682–19692.
7 Q. Liu, Q. Sun, C. Wei, X. Li, S. Yu, J. Li and Y. Chen, High performance and wearable hazardous gases sensor based on n-n heterojunction film of NGO and tetrakis(1-pyrenyl)porphyrin, *J. Hazard. Mater.*, 2021, **419**, 126460.
8 A. G. Martynov, Y. Horii, K. Katoh, Y. Bian, J. Jiang, M. Yamashita and Y. G. Gorbunov, Rare-earth based tetrapyrrolic sandwiches: chemistry, materials and applications, *Chem. Soc. Rev.*, 2022, **51**, 9262–9339, DOI: **10.1039/D2CS00559J**.
9 J. Jiang and D. K. P. Ng, A decade journey in the chemistry of sandwich-type tetrapyrrolato–rare earth complexes, *Acc. Chem. Res.*, 2008, **42**, 79–88.
10 Y. Chen, W. Su, M. Bai, J. Jiang, X. Li, Y. Liu, L. Wang and S. Wang, High performance organic field-effect transistors based on amphiphilic tris(phthalocyaninato) rare earth triple-decker complexes, *J. Am. Chem. Soc.*, 2005, **127**, 15700–15701.
11 J. Gao and G. Lu, J. kan, Y. Chen and M. Bouvet, Solution-processed thin films based on sandwich-type mixed (phthalocyaninato)(porphyrinato) europium triple-deckers: Structures and comparative performances in ammonia sensing, *Sens. Actuators, B*, 2012, **166–167**, 500–507.
12 S. Gai, B. Wang, X. Wang, R. Zhang, S. Miao and Y. Wu, Ultrafast NH_3 gas sensor based on phthalocyanine-optimized non-covalent hybrid of carbon nanotubes with pyrrole, *Sens. Actuators, B*, 2022, **357**, 131352.
13 J. Gao, D. Li and Y. Chen, Controllable self-assembly of sandwich-type mixed (phthalocyaninato)(porphyrinato) rare earth triple-decker complexes, *J. Inorg. Organomet. Polym. Mater.*, 2011, **21**, 876–880.
14 A. V. Kazak, M. A. Marchenkova, K. S. Khorkov, D. A. Kochuev, A. V. Rogachev, I. V. Kholodkov, N. V. Usol'tseva, M. S. Savelyev and A. Y. Tolbin, Ultrathin Langmuir–Schaefer films of slipped-cofacial J-type phthalocyanine dimer: Supramolecular organization, UV/Vis/NIR study and nonlinear absorbance of femtosecond laser radiation, *Appl. Surf. Sci.*, 2021, **545**, 148993.
15 W. Su, J. Jiang, K. Xiao, Y. Chen, Q. Zhao, G. Yu and Y. Liu, Thin-film transistors based on Langmuir–Blodgett films of heteroleptic bis (phthalocyaninato) rare earth complexes, *Langmuir*, 2005, **21**, 6527–6531.
16 Y. Chen, M. Bouvet, T. Sizun, Y. Gao, C. Plassard, E. Lesniewska and J. Jiang, Facile approaches to build ordered amphiphilic tris(phthalocyaninato) europium triple-decker complex thin films and their comparative performances in ozone sensing, *Phys. Chem. Chem. Phys.*, 2010, **12**, 12851–12861.
17 R. Wang, R. Li, Y. Li, X. Zhang, P. Zhu, P.-C. Lo, D. K. P. Ng, N. Pan, C. Ma, N. Kobayashi and J. Jiang, Controlling the nature of mixed (phthalocyaninato)(porphyrinato) rare-earth (III) double-decker complexes: the effects of nonperipheral alkoxy substitution of the phthalocyanine ligand, *Chem. – Eur. J.*, 2006, **12**, 1475–1485.
18 X. Kong, Z. Dong, Y. Wu, X. Li, Y. Chen and J. Jiang, High sensitive ambipolar response towards oxidizing NO_2 and reducing NH_3 based on bis(phthalocyaninato) europium semiconductors, *Chin. J. Chem.*, 2016, **34**, 975–982.
19 Y. Chen, X. Kong, G. Lu, D. Qi, Y. Wu, X. Li, M. Bouvet, D. Sun and J. Jiang, The lower rather than higher density charge carrier determines the NH_3-sensing nature and sensitivity of ambipolar organic semiconductors, *Mater. Chem. Front.*, 2018, **2**, 1009–1016.
20 Z. Liu, A. A. Yasseri, J. S. Lindsey and D. F. Bocian, Molecular memories that survive silicon device processing and real-world operation, *Science*, 2003, **302**, 1543–1545.
21 Y. Zhang, X. Cai, Y. Bian and J. Jiang, Organic semiconductors of phthalocyanine compounds for field effect transistors (FETs), *Struct. Bonding*, 2010, **135**, 275–322.
22 K. Katoh, Y. Yoshida, M. Yamashita, H. Miyasaka, B. K. Breedlove, T. Kajiwara, S. Takaishi, N. Ishikawa, H. Isshiki, Y. Zhang, T. Komeda, M. Yamagishi and J. Takeya, Direct observation of lanthanide(III)-phthalocyanine molecules on Au(111) by using scanning tunneling microscopy and scanning tunneling spectroscopy and thin-film field-effect transistor properties of Tb(III)- and Dy(III)-phthalocyanine molecules, *J. Am. Chem. Soc.*, 2009, **131**, 9967–9976.
23 Y. Chen, D. Li, N. Yuan, J. Gao, R. Gu, G. Lu and M. Bouvet, Tuning the semiconducting nature of bis(phthalocyaninato) holmium complexes via peripheral substituents, *J. Mater. Chem.*, 2012, **22**, 22142–22149.
24 I. Berg, L. Hale, M. Carmiel-Kostan, F. D. Toste and E. Gross, Using silyl protecting group to enable post-deposition C–C coupling reactions of alkyne-functionalized N-heterocyclic carbene monolayers on Au surfaces, *Chem. Commun.*, 2021, **57**, 5342–5345.
25 Y. Dong, J. Bi, S. Zhang, D. Zhu, D. Meng and S. Ming, Palladium supported on N-Heterocyclic carbene functionalized hydroxyethyl cellulose as a novel and efficient catalyst for the Suzuki reaction in aqueous media, *Appl. Surf. Sci.*, 2020, **531**, 147392.
26 G. Li, S. Liu, Y. Sun, W. Lou, Y.-F. Yang and Y. She, N-Heterocyclic carbene-based tetradentate platinum(II)

complexes for phosphorescent OLEDs with high brightness, *J. Mater. Chem. C*, 2022, **10**, 210–218.

27 E. Peris, Smart N-heterocyclic carbene ligands in catalysis, *Chem. Rev.*, 2018, **118**, 9988–10031.

28 V. E. Pushkarev, M. O. Breusova, E. V. Shulishov and Y. V. Tomilov, Selective synthesis and spectroscopic properties of alkyl-substituted lanthanide(III) mono-, di-, and triphthalocyanines, *Russ. Chem. Bull.*, 2005, **54**, 2087–2093.

29 E. N. Tarakanova, P. A. Tarakanov, A. O. Simakov, T. Furuyama, N. Kobayashi, D. V. Konev, O. A. Goncharov, S. A. Trashin, K. D. Wael, I. V. Sulimenkov, V. V. Filatov, V. I. Kozlovskiy, L. G. Tomilova, P. A. Stuzhin and V. E. Pushkarev, Synthesis and characterization of heteroleptic rare earth double-decker complexes involving tetradiazepinoporphyrazine and phthalocyanine macrocycles, *Dalton Trans.*, 2021, **50**, 6245–6255.

30 E. N. Tarakanova, S. A. Trashin, A. O. Simakov, T. Furuyama, A. V. Dzuban, L. N. Inasaridze, P. A. Tarakanov, P. A. Troshin, V. E. Pushkarev, N. Kobayashi and L. G. Tomilova, Double-decker bis(tetradiazepinoporphyrazinato) rare earth complexes: crucial role of intramolecular hydrogen bonding, *Dalton Trans.*, 2016, **45**, 12041–12052.

31 M. Bouvet, H. Xiong and V. Parra, Molecular semiconductor-doped insulator (MSDI) heterojunctions: oligothiophene/bisphtalocyanine ($LuPc_2$) and perylene/bisphthalocyanine as new structures for gas sensing, *Sens. Actuators, B*, 2010, **145**, 501–506.

32 M. Kasha, H. R. Rawls and M. A. El-Bavoumi, The exciton model in molecular spectroscopy, *Pure Appl. Chem.*, 1965, **11**, 371–392.

33 N. An, Y. Shi, J. Feng, D. Li, J. Gao, Y. Chen and X. Li, N-channel organic thin-film transistors based on a soluble cyclized perylene tetracarboxylic diimide dimer, *Org. Electron.*, 2013, **14**, 1197–1203.

34 T. J. Prosa, M. J. Winokur, J. Moulton, P. Smith and A. J. Heeger, X-ray structural studies of poly(3-alkylthiophenes): an example of an inverse comb, *Macromolecules*, 1992, **25**, 4364–4372.

35 M. Yoneyama, M. Sugi, M. Saito, K. Ikegami, S. Kuroda and S. Iizima, Photoelectric properties of copper phthalocyanine Langmuir-Blodgett film, *Jpn. J. Appl. Phys.*, 1986, **25**, 961.

36 W.-T. Koo, S.-J. Choi, S.-J. Kim, J.-S. Jang, H. L. Tuller and I.-D. Kim, Heterogeneous sensitization of metal–organic framework driven metal@metal oxide complex catalysts on an oxide nanofiber scaffold toward superior gas sensors, *J. Am. Chem. Soc.*, 2016, **138**, 13431–13437.

37 M. L. Tang, A. D. Reichardt, P. Wei and Z. Bao, Correlating carrier type with frontier molecular orbital energy levels in organic thin film transistors of functionalized acene derivatives, *J. Am. Chem. Soc.*, 2009, **131**, 5264–5273.

38 J. Kan, Y. Chen, D. Qi, Y. Liu and J. Jiang, High-performance air-stable ambipolar organic field-effect transistor based on tris(phthalocyaninato) europium (III), *Adv. Mater.*, 2012, **24**, 1755–1758.

39 D. Gao, X. Zhang, X. Kong, Y. Chen and J. Jiang, (TFPP)Eu[Pc(OPh)$_8$]Eu[Pc(OPh)$_8$]/CuPc two-component bilayer heterojunction-based organic transistors with high ambipolar performance, *ACS Appl. Mater. Interfaces*, 2015, **7**, 2486–2493.

40 X. Wang, H. Wang, X. Ding, X. Wang, X. Li and Y. Chen, High performance room-temperature NO_2 sensors based on microstructures self-assembled from n-type phthalocyanines: Effect of fluorine–hydrogen bonding and metal–ligand coordination on morphology and sensing performance, *Org. Electron.*, 2017, **50**, 389–396.

41 R. D. Yang, J. Park, C. N. Colesniuc, I. K. Schuller, J. E. Royer, W. C. Trogler and A. C. Kummel, Analyte chemisorption and sensing on n- and p-channel copper phthalocyanine thin-film transistors, *J. Chem. Phys.*, 2009, **130**, 164703.

42 G. Lu, K. Wang, X. Kong, H. Pan, J. Zhang, Y. Chen and J. Jiang, Binuclear phthalocyanine dimer-containing Yttrium double-decker ambipolar semiconductor with sensitive response toward oxidizing NO_2 and reducing NH_3, *ChemElectroChem*, 2018, **5**, 605–609.

43 K. Potje-Kamloth, Semiconductor junction gas sensors, *Chem. Rev.*, 2008, **108**, 367–399.

44 S. Liu, H. Wang, X. Wang, S. Li, H. Liu, Y. Chen and X. Li, Diverse sensor responses from two functionalized tris(phthalocyaninato)europium ambipolar semiconductors towards three oxidative and reductive gases, *J. Mater. Chem. C*, 2019, **7**, 424.

45 X. Duan, Y. Zhang, H. Wang, F. Dai, G. Yang and Y. Chen, A phthalocyanine sensor array based on sensitivity and current changes for highly sensitive identification of three toxic gases at ppb levels, *New J. Chem.*, 2020, **44**, 13240–13248.

46 C. M. Hussain, S. K. Shukla and G. M. Joshi, *Functionalized Nanomaterials Based Devices for Environmental Applications*, Elsevier, 2021.